THE JOURNAL OF PHYSICAL CHEMISTRY B
A JOURNAL OF THE AMERICAN CHEMICAL SOCIETY

pubs.acs.org/JPCB

Article

Transition Path Sampling Based Free Energy Calculations of Evolution's Effect on Rates in β-Lactamase: The Contributions of Rapid Protein Dynamics to Rate

Published as part of The Journal of Physical Chemistry B special issue "At the Cutting Edge of Theoretical and Computational Biophysics".

Clara F. Frost, Dimitri Antoniou, and Steven D. Schwartz*

Cite This: J. Phys. Chem. B 2024, 128, 11658−11665

Read Online

ACCESS | Metrics & More | Article Recommendations

ABSTRACT: β-Lactamases are one of the primary enzymes responsible for antibiotic resistance and have existed for billions of years. The structural differences between a modern class A TEM-1 β-lactamase compared to a sequentially reconstructed Gram-negative bacteria β-lactamase are minor. Despite the similar structures and mechanisms, there are different functions between the two enzymes. We recently identified differences in dynamics effects that result from evolutionary changes that could potentially account for the increase in substrate specificity and catalytic rate. In this study, we used transition path sampling-based calculations of free energies to identify how evolutionary changes found between an ancestral β-lactamase, and its extant counterpart TEM-1 β-lactamase affect rate.

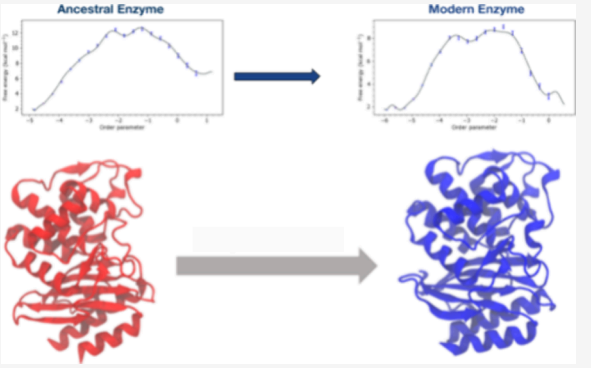

INTRODUCTION

Progress in protein engineering requires understanding the details of enzymatic function, such as how a single mutation affects the rate of catalysis, since small changes in the structure of an enzyme can significantly affect the catalytic rate.[1] Studying the natural evolution of enzymes can provide insight into these details and holds promise for advancing the field of protein engineering. For the most part, this entails the comparison of modern enzymes with ancestral reconstructions. The most successful artificial enzymes with the highest levels of catalytic rates have been obtained by directed evolution.[2] Several factors contribute to why these evolved artificial enzymes are successful, and in an earlier study of the retro-aldolase series, we identified the importance of fast motions that are coupled to the chemical step.[3] We had also identified such fast rate-promoting motions in other enzymatic systems, along with how they may be modified by mutation and mass changes.[4−6] The results of the directed-evolution retro-aldolase study encouraged investigation in naturally evolved enzymes for the possible evolutionary emergence of rapid dynamics that affect the catalytic rate.

In a previous study, we identified differences in the presence of rapid dynamics between a Precambrian class-A Gram-negative bacterial β-lactamase (GNCA) found via sequence reconstruction, and its modern counterpart, TEM-1 β-lactamase.[7] The availability of reconstructed ancestral enzymes has greatly contributed to understanding the dynamic properties among a variety of time scales that are present throughout evolution.[8−11] We identified the reaction coordinates in the two systems using transition path sampling (TPS), studied the motions of residues that participate in the reaction coordinate, and found differences between the two enzymes in dynamics during two distinct parts of the chemical reaction. We found that these differences were consistent with the location in time of peaks of the active site electric fields during the chemical step: in the ancestral enzyme (where dynamics does not play a role) the electric field peaks at the transition state, while in the modern enzyme the changes in the electric field correlate with the evolving distance between Ala237 and a substrate oxygen. However, how such subps motions affect free energies to reaction had been elusive. In the present study, we have performed TPS-based free energy simulations[12] to calculate the free energy barriers for two chemical reaction steps in both the ancestral GNCA β-

Received: October 2, 2024
Revised: November 6, 2024
Accepted: November 11, 2024
Published: November 13, 2024

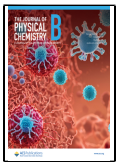

https://doi.org/10.1021/acs.jpcb.4c06689
J. Phys. Chem. B 2024, 128, 11658−11665

lactamase and the modern TEM-1 β-lactamase, and have shown how the presence - or absence - of rapid dynamics affects the free energy barriers in the acylation portion of this enzyme's catalytic function.

The evolution of β-lactamase over the past 2−3 billion years has been extensively studied, with the crystal structures of several Precambrian β-lactamases generated through ancestral sequence reconstruction.[13−15] In general, ancestral enzymes are known to be slower catalysts, have larger active sites, and can accommodate a wide range of substrates.[9,14] This class of enzymes is extremely well studied because β-lactamase is primarily responsible for antibiotic resistance.

The ancestral GNCA enzyme and modern TEM-1 β-lactamase in this study have nearly identical structures as shown in Figure 1. While there are several ancestral β-lactamase reconstructions and their extant counterparts, we chose this specific pair due to the availability of a substrate-bound structure in the Protein Data Bank, and the high degree of similarity between them. Additionally, TEM-1 β-lactamase is known as a useful system for exploring novel protein engineering techniques due to the availability of a detailed evolution pathway. There are hundreds of amino acid mutations between the two proteins, but only one is found in the active site: the Thr237 residue in the ancestral enzyme is Ala237 in the modern, and this residue plays an important role in the chemical reaction. Known functional differences between the two structures include the substrate specificity of the modern enzyme, whereas the ancestral enzyme can accommodate a multitude of substrates.[13,15] Despite these differences, identical overall chemical mechanisms were found in both enzymes. Experimental studies on both enzymes showed that the modern enzyme's catalytic rate is 2 orders of magnitude higher than that of the ancestral enzyme.[16] In this paper, we address one of the causes of this rate difference.

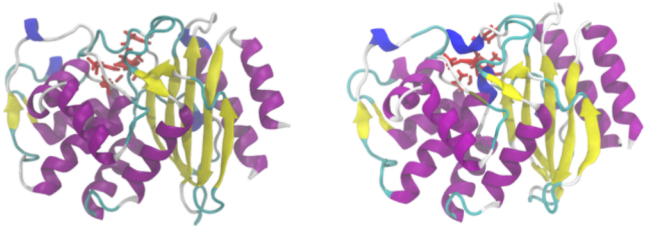

Figure 1. Protein structure of the ancestral GNCA (left) and modern TEM-1 β-lactamases (right) with respect to their secondary structures (multicolored sequences). The substrate benzylpenicillin is shown in red.

Conformational motions, and most recently, rapid femtosecond motions, have been extensively studied within these two systems.[15,16] Ozkan et al. explored the evolutionary trajectory in terms of the hinge-shift mechanisms in the two enzymes.[15,16] These studies revealed that specific conformational motions evolved to make changes in substrate specificity and rate enhancements. By examining these specific motions, both conformational and the much faster subpicosecond dynamics, we can identify specific residue mutations that are at least partially responsible for evolutionary changes in enzyme function.

COMPUTATIONAL METHODS

System Preparation. The crystallized structures were obtained from the Protein Data Bank with the ancestral PDB ID: 4b88 and the modern PDB ID: 1fqg. TEM-1 β-lactamase contained the benzylpenicillin substrate, which was then copied into the ancestral GNCA apo-form using Schrödinger Maestro.[17] Both crystal structures were in the tetrahedral intermediate formation, so minimization was employed to return the structure to the prereactant state, thus allowing us to study the "preacylation" step. All simulations were performed using the CHARMM42 program.[18,19] The TIP3P water model[20] was used to solvate the protein, followed by neutralization with nine sodium ions placed throughout each system. Then both systems underwent minimization through 50 steps of steepest descent, followed by 2000 steps of the adopted basis Netwon-Raphson (ABNR) method.

The QM/MM method was applied to partition each system into a QM region, treated with the semiempirical method AM1, and an MM region, adhering to the CHARMM36 force field.[21] The general hybridized orbital (GHO) method was used to treat the boundary atoms.[22] The QM region included benzylpenicillin, as well as residues Ser70, Ser130, Glu166, Lys73, and the catalytic water. The benzylpenicillin parameters were generated using Discovery Studio.[23] Once the QM and MM regions were patched together, both systems were then slowly heated to 300 K, starting with 15 ps of harmonic constraints (without the TIP3P water molecules and hydrogen atoms) followed by 5 ps of small harmonic constraints, then 10 ps, with harmonic restraints on the QM heavy atoms. The SHAKE algorithm was applied for the hydrogen atoms. Equilibration was performed with QM on for 15 ps with harmonic constraints, then for 60 ps with the harmonic constraints removed. The second step, the acylenzyme formation, started with the final structure of the tetrahedral intermediate from a reactive TPS trajectory and then was equilibrated to generate the structure required for step 2.

Free energy profiles were calculated using the transition path sampling based method[24] for both mechanistic steps for the ancestral and modern enzymes. The calculations required reactive trajectories as guiding trajectories for the window samplings, which were taken from ensembles of reactive trajectories. These ensembles were generated in a previous study (Frost, et. al 2024)[7] through transition path sampling (TPS).[25] TPS generates an unbiased ensemble of reactive trajectories that illustrate the mechanistic path the system takes to get from the reactant state to the product state. Only accepted trajectories that connect the two stable states, reactant and product, are kept to form the transition path ensemble. Hundreds of reactive trajectories were generated, with further details on the method of transition path sampling found in that manuscript. With the reactive trajectories for both steps, we were able to then apply the free energy TPS method to calculate the free energy profiles.

The free energy barriers were calculated for both ancestral and modern enzymes, and for both step 1: formation of the tetrahedral intermediate; and step 2: acylation of the tetrahedral intermediate. The order parameters were defined for each reaction that can distinguish between the reactant and product states, as seen in Figure 2.

Step 1: Formation of the Tetrahedral Intermediate. The order parameter ζ for both enzymes is the linear combination of 3 bond-forming and 2 bond-breaking distances: $\zeta = d(\mathrm{OGX}$

https://doi.org/10.1021/acs.jpcb.4c06689
J. Phys. Chem. B 2024, 128, 11658−11665

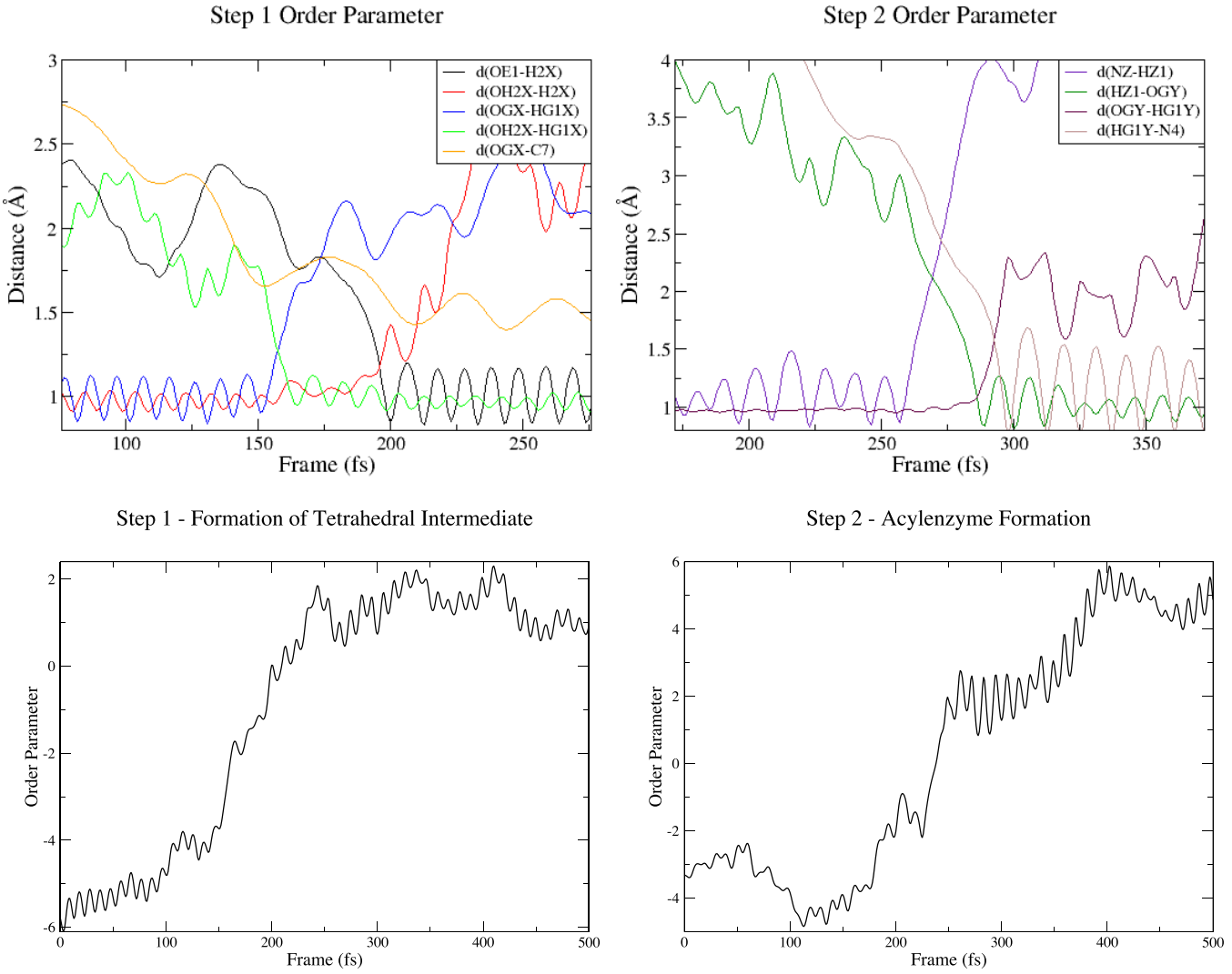

Figure 2. Top shows the order parameter distances for both steps. Step 1 has the bonds breaking (OH2X-H2X) and (OGX-HG1X) and bonds forming (OE1-H2X), (OH2X-HG1X), and (OGX-C7). Step 2 shows bonds (NZ-HZ1) and (OGY-HG1Y) breaking and bonds (HZ1-OGY), (HG1Y−N4) forming. Underneath the bond distances shows the order parameters as the linear combination of bonds breaking and bonds forming for both steps that distinguish the reactant state and product states.

− HG1X) − d(HG1X − OH2X) + d(OH2X − H2X) − d(OE1 − H2X) − d(OGX − C7), with the bond distances of interest shown in Figure 2 for both steps. The window for each order parameter was determined by taking the transition state identified through committor analysis in the previous study and using the range ±100 fs from the transition state time frame. A reactive trajectory for each system from the TPS ensemble was used for the equilibrium sampling. Configurations are sampled for order parameter values [-4.9, 1.17] for the ancestral and [-6.02, 0.50] for the modern.

Step 2: Acylation of the Tetrahedral Intermediate. The order parameter ζ for the second step only consists of the second two proton transfers, where ζ = d(NZ − HZ1) − d(HZ1 − OGY) + d(OGY − HG1Y) − d(HG1Y − N4). In the ancestral enzyme, the initial proton transfer from Glu166 to Lys73 happens within the first 5 fs of a reactive trajectory, so to maintain the same process for both systems the order parameter contains only the second two transfers. The order parameter minimum and maximum for the ancestral enzyme was [-4.41, 1.89] and the modern TEM-1 enzyme was [-6.18, 6.4]. The order parameter values were calculated the same way as in step 1, taking the transition state of each reactive trajectory and finding the values corresponding to the frame ±100 fs from the transition state.

Free Energy Calculations. The order parameter ranges were then divided into 20 windows, with 0.08 A° overlap between neighboring windows. Each window (i) obtains a set of order parameter values ($[\zeta_i^{min}, \zeta_i^{max}]$), in which a time slice is chosen to initiate sampling of configurations. Using the shooting algorithm,[25,26] short 20 fs trajectories are generated by perturbing the momenta of all atoms in the enzymatic system and the system is propagated 10 fs backward and 10 fs forward from the shooting point (initial time slice). 2000 trajectories were generated to thoroughly sample each window, and the converged probability distribution of the order parameter was obtained as normalized histograms. The free energy is calculated within each window by Boltzmann inversion $F_i = -k_B T \log (w_i)$, where w_i is the probability of the occupation of the specific window (i), and then combined to obtain the continuous total free energy profile for the reaction. Bootstrapping analysis was used to calculate the

https://doi.org/10.1021/acs.jpcb.4c06689
J. Phys. Chem. B 2024, 128, 11658−11665

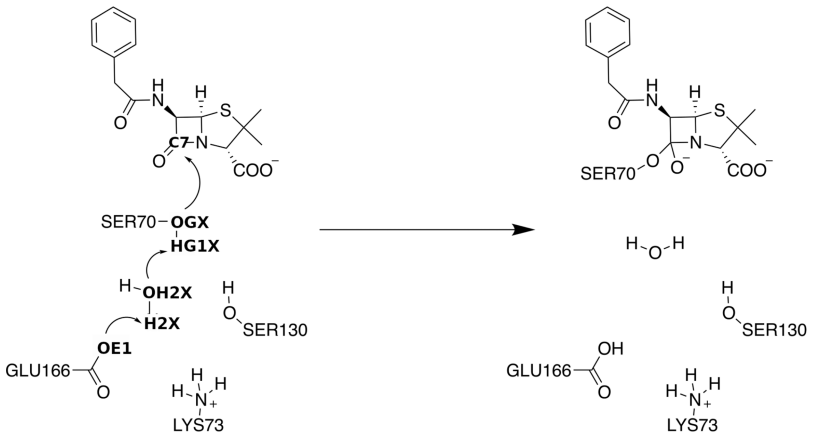

Figure 3. First step is the "preacylation" step. Ser70 loses a proton to the catalytic water, which then donates a proton to the Glu166 residue, leaving Ser70 to attack the β-lactam carbonyl carbon C7. The atoms involved in these steps are labeled.

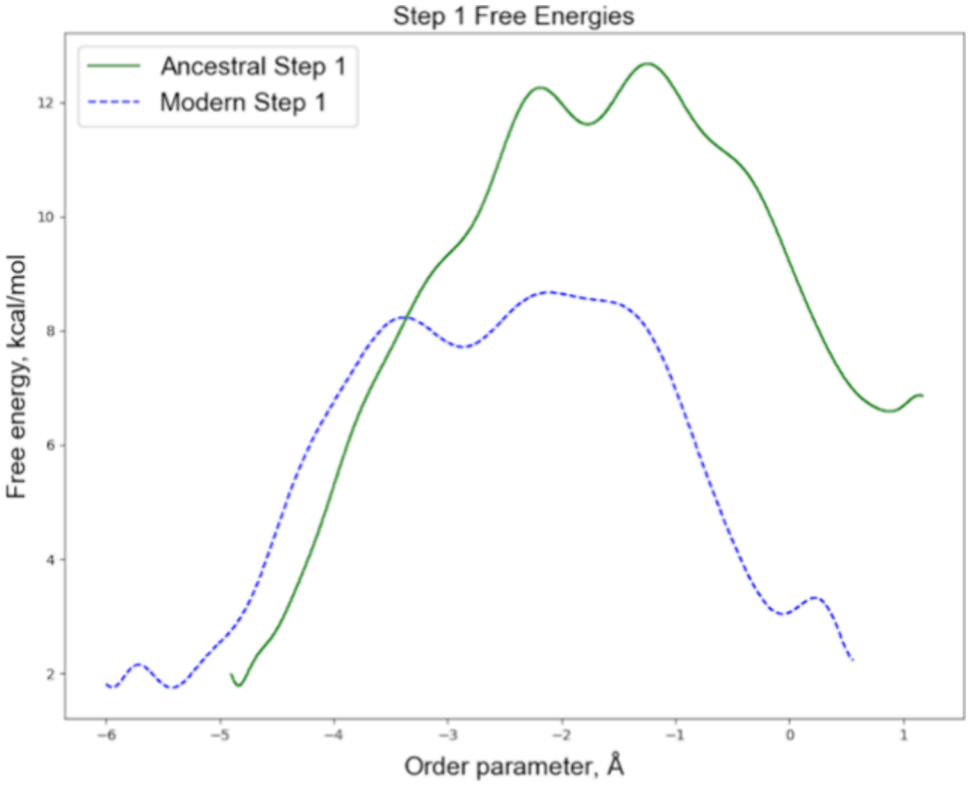

Figure 4. Free energy barriers calculated using the TPS method for the first step in the acylation mechanism. The ancestral enzyme (green) and modern enzyme (blue).

standard deviations for the populations of configurations sampled within each window.[27]

RESULTS AND DISCUSSION

β-Lactamase breaks down β-lactam antibiotics in 2 distinct chemical processes: acylation and deacylation. In this study we focus on the acylation mechanism, which, in turn, consists of two steps.

Step 1. There is a debate on the mechanistic pathway for the first step, which forms the tetrahedral intermediate before the acylation. Experimental and computational evidence provide that the Ser70 residue is activated by the Glu66 residue,[28,29] but other groups have suggested that it is actually the Lys73 residue in the active site that activates the mechanism.[30,31] In this work we found the mechanism that was originally proposed, activation through Glu166, for both the ancestral and modern enzymes. This mechanism emerged through unbiased generation by TPS of reactive trajectories for both the ancestral and the modern. This pathway is shown in Figure 3:

The first step involves two proton transfers and a nucleophilic attack. The Ser70 oxygen, OGX, attacks the β-lactam carbonyl on benzylpenicillin to form the tetrahedral intermediate. The results from our previous TPS study showed a significant presence of dynamics in the modern enzyme for this step. The ancestral enzyme remains static for the preacylation step, but in the modern enzyme, the mutated residue Ala237 moves toward the oxygen on the β-lactam

https://doi.org/10.1021/acs.jpcb.4c06689
J. Phys. Chem. B 2024, 128, 11658−11665

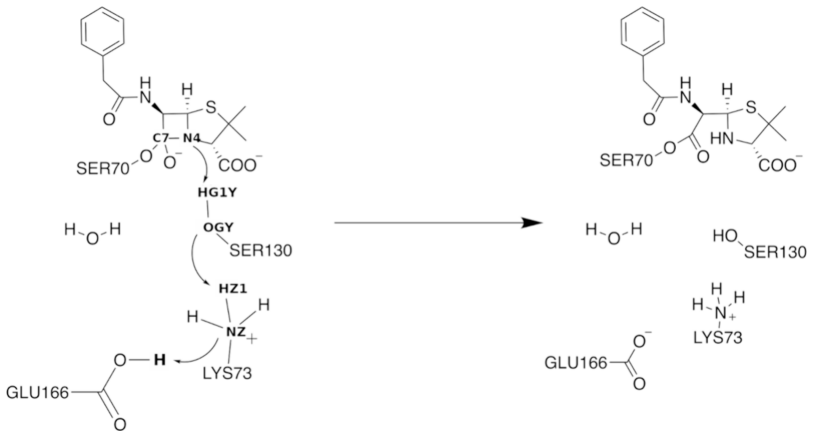

Figure 5. Acylation mechanism with three proton transfers resulting in the breaking of the β-lactam ring between C7 and N4.

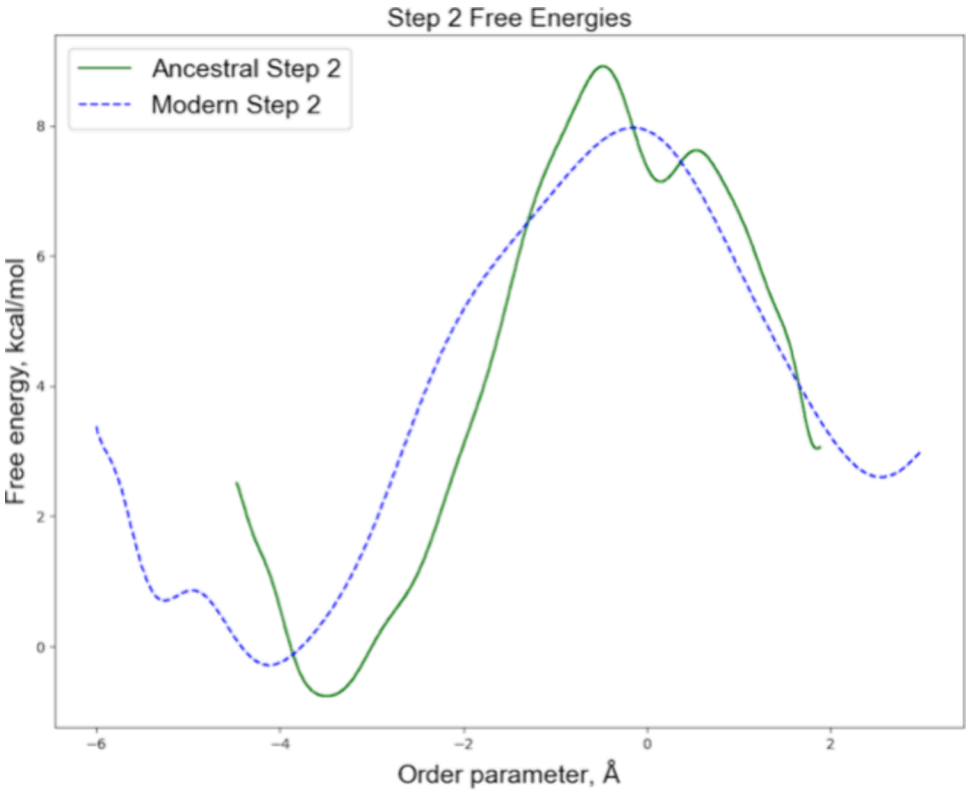

Figure 6. Free energy profiles as a function of the order parameter for the second acylation step. The ancestral enzyme (green) and the modern enzyme (blue).

carbonyl less than 100 fs before the formation of the transition state. The backbone amide hydrogen bonds to the O8 oxygen of the β-lactam carbonyl, and the breaking of the bond polarizes the carbonyl preparing it for the nucleophilic attack of the Ser70 oxygen. This is not seen in the ancestral enzyme; in fact, the active site remains static with less than 0.5 Å motion of the reaction coordinate residues. The free energy profiles we calculated for the "preacylation" step in the ancestral and modern enzymes are shown in Figure 4.

The free energy barrier is 10.5 ± 0.18 kcal/mol in the ancestral enzyme and 6.9 ± 0.16 kcal/mol in the modern enzyme. We have previously shown that the presence of new rapid dynamics exists in the modern enzyme,[7] which is at least partially responsible for this free energy barrier reduction. We should point out that in our earlier study of this system, the presence of fast dynamics in the modern enzyme in this step correlated with the peak in the electric fields in the active site corresponding with the fluctuations of the Ala237 residue.

Step 2. In the second step, the ancestral enzyme exhibits very modest dynamics, and any rapid dynamics in the modern enzyme occurs more than 100 fs before the system reaches the transition state. The mechanism for the second step is the same for both systems and contains three proton transfers as illustrated in Figure 5:

In the ancestral enzyme, the previously static active site shows movement of the Thr237 residue toward the O8 oxygen on the β-lactam carbonyl before the formation of the transition state. In contrast, the modern enzyme has a static Ala237 residue, with the remaining reaction coordinate residues also remaining static near the transition state. In the modern

https://doi.org/10.1021/acs.jpcb.4c06689
J. Phys. Chem. B 2024, 128, 11658−11665

enzyme, one active site residue moves close to the substrate's carboxylate side chain, but after the transition state. The free energy barriers for this second step are shown below in Figure 6.

The free energy barrier in the ancestral enzyme is 9.6 ± 0.15 kcal/mol and for the modern enzyme we find 7.7 ± 0.14 kcal/mol. The first and second step in both proteins have roughly similar free energy barriers. Roughly 10 kcal/mol for the first and second steps in the ancestral, and similarly around 7.5 kcal/mol for the modern. A 2.5 kcal/mol difference corresponds to roughly 4.2 kT, which in turn corresponds to 1.8 orders of magnitude—a fairly close approximation of the observed 2 order of magnitude difference. Of course, slower motions are important, and these rapid promoting vibration compressions are not the end of the story, but this level of at least rough agreement is in fact remarkable.

In our earlier study, we found that the active site electric field in the second acylation step correlates to the fluctuations in the ancestral enzyme, where the field peaks before the transition state. In the first acylation step, with no dynamics present, the field peaks at the transition state corresponding to the chemical reaction itself. The free energy profiles described here show the same trend.

CONCLUSIONS

The structure and mechanism of the modern TEM-1 β-lactamase are nearly identical to those of the ancestral GNCA enzyme. Despite this, the modern enzyme exhibits increased enzymatic efficiency and substrate specificity. Free energy profiles reveal that the mobility of the active sites is among the evolutionary changes that affect enzyme function. Modest changes in the protein body and a single mutation T237A in the active site significantly influence substrate specificity and the catalytic rate, with changes in dynamics that correlate with these effects. Studies have also shown that the A237T mutation in the TEM-1 enzyme increases antibiotic resistance to a wider range of β-lactam antibiotics.[32,33] Ancestral sequence reconstruction is a powerful tool that provides the opportunity to study evolution biochemistry, and determine the evolutionary changes of structure and function, and trace these changes through time.[34−38] More information on the mutational pathway leading to the TEM-1 modern enzyme would be illuminating, and specific point mutations within these β-lactamase systems are already being analyzed to identify effects on flexibility, allostery, and predicting mutational effects.[16,39−49]

Comparing the two steps for the acylation mechanism, it is evident that the preacylation step must occur before the acylation of the tetrahedral intermediate. The lower free energy barrier in the first step is likely influenced by the rapid dynamics in the modern enzyme, which is absent in the ancestral. The higher barrier in the ancestral may be related to its ability to catalyze a variety of reactions with different substrates. It must be remembered that in regular TPS simulations (unlike the free energy computations reported in this manuscript) only reactive trajectories become part of the transition path ensemble. Thus, reactive trajectories for the modern enzyme can be generated without protein dynamics because the needed dynamics have already happened in the first step. In the ancestral enzyme, this is not the case, and the system has to "wait" for the needed compression for the second step to occur. Once the first step occurs in the ancestral enzyme, the second step is facilitated by the fluctuations of catalytic residues, driving the reaction forward. These changes, particularly responsible from a single mutation in the active site, provide insight into the evolutionary changes in substrate specificity.

The free energy barrier calculations provide insights into the evolution of the catalytic rate. For the preacylation step, the ancestral enzyme shows a barrier that is 3.6 kcal/mol higher than the modern enzyme. The catalytic rate of the modern enzyme is 2 orders of magnitude higher than that of the ancestral enzyme. These findings suggest that the rapid dynamics impact the catalytic rate to a highly significant degree. In fact, the computations presented here are one of the first direct correlations of promoting vibration dynamics to experimentally measured rates in evolved proteins. Additional influences are certainly expected to be due to the evolved conformational motions observed in Ozkan's work. For the rapid dynamics, and promoting vibrations, the only experimental probe of the impact of promoting vibrations is mutational experiments.[50,51] The results from this study show a direct correlation between rapid promoting vibrations and measured experimental rates.

AUTHOR INFORMATION

Corresponding Author

Steven D. Schwartz − *Department of Chemistry & Biochemistry, University of Arizona, Tucson, Arizona 85721, United States;* orcid.org/0000-0002-0308-1059; Phone: (520) 621-6363; Email: sschwartz@arizona.edu

Authors

Clara F. Frost − *Department of Chemistry & Biochemistry, University of Arizona, Tucson, Arizona 85721, United States*

Dimitri Antoniou − *Department of Chemistry & Biochemistry, University of Arizona, Tucson, Arizona 85721, United States*

Complete contact information is available at: https://pubs.acs.org/10.1021/acs.jpcb.4c06689

Notes

The authors declare no competing financial interest.

ACKNOWLEDGMENTS

All computer simulations were performed at the University of Arizona High Performance Computing Center, on a Penguin Altus XE2242 supercomputer. This research was supported through the NIH grant R35GM145213.

REFERENCES

(1) Romero, P. A.; Arnold, F. H. Exploring Protein Fitness Landscapes by Directed Evolution. *Nat. Rev. Mol. Cell Biol.* **2009**, *10* (12), 866−876.

(2) Brustad, E. M.; Arnold, F. H. Optimizing Non-Natural Protein Function with Directed Evolution. *Curr. Opin. Chem. Biol.* **2011**, *15* (2), 201−210.

(3) Schafer, J. W.; Zoi, I.; Antoniou, D.; Schwartz, S. D. Optimization of the Turnover in Artificial Enzymes via Directed Evolution Results in the Coupling of Protein Dynamics to Chemistry. *J. Am. Chem. Soc.* **2019**, *141* (26), 10431−10439.

(4) Masterson, J. E.; Schwartz, S. D. Changes in Protein Architecture and Subpicosecond Protein Dynamics Impact the Reaction Catalyzed by Lactate Dehydrogenase. *J. Phys. Chem. A* **2013**, *117* (32), 7107−7113.

(5) Schwartz, S. D. Protein Dynamics and the Enzymatic Reaction Coordinate. In *Dynamics in Enzyme Catalysis*; Klinman, J.; Hammes-

Schiffer, S., Eds.; Topics in Current Chemistry; Springer Berlin Heidelberg: Berlin, Heidelberg, 2013; Vol. *337*, pp 189−208. .
(6) Schwartz, S. D.; Schramm, V. L. Enzymatic Transition States and Dynamic Motion in Barrier Crossing. *Nat. Chem. Biol.* **2009**, *5* (8), 551−558.
(7) Frost, C. F.; Antoniou, D.; Schwartz, S. D. The Evolution of the Acylation Mechanism in β-Lactamase and Rapid Protein Dynamics. *ACS Catal.* **2024**, *14*, 13640−13651.
(8) Gumulya, Y.; Gillam, E. M. J. Exploring the Past and the Future of Protein Evolution with Ancestral Sequence Reconstruction: The 'Retro' Approach to Protein Engineering. *Biochem. J.* **2017**, *474* (1), 1−19.
(9) Perez-Garcia, P.; Kobus, S.; Gertzen, C. G. W.; Hoeppner, A.; Holzscheck, N.; Strunk, C. H.; Huber, H.; Jaeger, K.-E.; Gohlke, H.; Kovacic, F.; et al. A Promiscuous Ancestral Enzyme's Structure Unveils Protein Variable Regions of the Highly Diverse Metallo-β-Lactamase Family. *Commun. Biol.* **2021**, *4* (1), 132.
(10) Petrović, D.; Risso, V. A.; Kamerlin, S. C. L.; Sanchez-Ruiz, J. M. Conformational Dynamics and Enzyme Evolution. *J. R. Soc. Interface* **2018**, *15* (144), 20180330.
(11) Modi, T.; Campitelli, P.; Heyden, M.; Ozkan, S. B. Correlated Evolution of Low-Frequency Vibrations and Function in Enzymes. *J. Phys. Chem. B* **2023**, *127* (3), 616−622.
(12) Balasubramani, S. G.; Korchagina, K.; Schwartz, S. Transition Path Sampling Study of Engineered Enzymes That Catalyze the Morita−Baylis−Hillman Reaction: Why Is Enzyme Design so Difficult? *J. Chem. Inf. Model.* **2024**, *64* (6), 2101−2111.
(13) Risso, V. A.; Gavira, J. A.; Mejia-Carmona, D. F.; Gaucher, E. A.; Sanchez-Ruiz, J. M. Hyperstability and Substrate Promiscuity in Laboratory Resurrections of Precambrian β-Lactamases. *J. Am. Chem. Soc.* **2013**, *135* (8), 2899−2902.
(14) Risso, V. A.; Martinez-Rodriguez, S.; Candel, A. M.; Krüger, D. M.; Pantoja-Uceda, D.; Ortega-Muñoz, M.; Santoyo-Gonzalez, F.; Gaucher, E. A.; Kamerlin, S. C. L.; Bruix, M.; et al. De Novo Active Sites for Resurrected Precambrian Enzymes. *Nat. Commun.* **2017**, *8* (1), 16113.
(15) Modi, T.; Risso, V. A.; Martinez-Rodriguez, S.; Gavira, J. A.; Mebrat, M. D.; Van Horn, W. D.; Sanchez-Ruiz, J. M.; Banu Ozkan, S. Hinge-Shift Mechanism as a Protein Design Principle for the Evolution of β-Lactamases from Substrate Promiscuity to Specificity. *Nat. Commun.* **2021**, *12* (1), 1852.
(16) Zou, T.; Risso, V. A.; Gavira, J. A.; Sanchez-Ruiz, J. M.; Ozkan, S. B. Evolution of Conformational Dynamics Determines the Conversion of a Promiscuous Generalist into a Specialist Enzyme. *Mol. Biol. Evol.* **2015**, *32* (1), 132−143.
(17) *Schrödinger Release 2023−3: Maestro*; Schrödinger, LLC: New York, NY, 2023.
(18) Brooks, B. R.; Bruccoleri, R. E.; Olafson, B. D.; States, D. J.; Swaminathan, S.; Karplus, M. CHARMM: A Program for Macromolecular Energy, Minimization, and Dynamics Calculations. *J. Comput. Chem.* **1983**, *4* (2), 187−217.
(19) Brooks, B. R.; Brooks, C. L.; Mackerell, A. D.; Nilsson, L.; Petrella, R. J.; Roux, B.; Won, Y.; Archontis, G.; Bartels, C.; Boresch, S.; et al. CHARMM: The Biomolecular Simulation Program. *J. Comput. Chem.* **2009**, *30* (10), 1545−1614.
(20) Jorgensen, W. L.; Chandrasekhar, J.; Madura, J. D.; Impey, R. W.; Klein, M. L. Comparison of Simple Potential Functions for Simulating Liquid Water. *J. Chem. Phys.* **1983**, *79* (2), 926−935.
(21) Vanommeslaeghe, K.; Hatcher, E.; Acharya, C.; Kundu, S.; Zhong, S.; Shim, J.; Darian, E.; Guvench, O.; Lopes, P.; Vorobyov, I.; et al. D. CHARMM General Force Field: A Force Field for Drug-like Molecules Compatible with the CHARMM All-atom Additive Biological Force Fields. *J. Comput. Chem.* **2010**, *31* (4), 671−690.
(22) Gao, J.; Amara, P.; Alhambra, C.; Field, M. J. A Generalized Hybrid Orbital (GHO) Method for the Treatment of Boundary Atoms in Combined QM/MM Calculations. *J. Phys. Chem. A* **1998**, *102* (24), 4714−4721.
(23) Biovia, D. S. (2019) *Discovery Studio Visualizer*; Accelrys Software Inc: San Diego.
(24) Balasubramani, S. G.; Schwartz, S. D. Transition Path Sampling Based Calculations of Free Energies for Enzymatic Reactions: The Case of Human Methionine Adenosyl Transferase and *Plasmodium Vivax* Adenosine Deaminase. *J. Phys. Chem. B* **2022**, *126* (29), 5413−5420.
(25) Bolhuis, P. G.; Chandler, D.; Dellago, C.; Geissler, P. L. TRANSITION PATH SAMPLING: Throwing Ropes Over Rough Mountain Passes, in the Dark. *Annu. Rev. Phys. Chem.* **2002**, *53* (1), 291−318.
(26) Dellago, C.; Bolhuis, P. G.; Geissler, P. L. Transition Path Sampling Methods. In *Computer Simulations in Condensed Matter Systems: From Materials to Chemical Biology Vol. 1*; Ferrario, M.; Ciccotti, G.; Binder, K., Eds.; Lecture Notes in Physics; Springer Berlin Heidelberg: Berlin, Heidelberg, 2006; Vol. *703*, pp 349−391. .
(27) Hub, J. S.; De Groot, B. L.; Van Der Spoel, D. G_wham—A Free Weighted Histogram Analysis Implementation Including Robust Error and Autocorrelation Estimates. *J. Chem. Theory Comput.* **2010**, *6* (12), 3713−3720.
(28) Minasov, G.; Wang, X.; Shoichet, B. K. An Ultrahigh Resolution Structure of TEM-1 β-Lactamase Suggests a Role for Glu166 as the General Base in Acylation. *J. Am. Chem. Soc.* **2002**, *124* (19), 5333−5340.
(29) Hermann, J. C.; Ridder, L.; Mulholland, A. J.; Höltje, H.-D. Identification of Glu166 as the General Base in the Acylation Reaction of Class A β-Lactamases through QM/MM Modeling. *J. Am. Chem. Soc.* **2003**, *125* (32), 9590−9591.
(30) Langan, P. S.; Vandavasi, V. G.; Cooper, C. J.; Weiss, K. L.; Ginell, S. L.; Parks, J. M.; Coates, L. Substrate Binding Induces Conformational Changes in a Class A β-Lactamase That Prime It for Catalysis. *ACS Catal.* **2018**, *8* (3), 2428−2437.
(31) Meroueh, S. O.; Fisher, J. F.; Schlegel, H. B.; Mobashery, S. Ab Initio QM/MM Study of Class A β-Lactamase Acylation: Dual Participation of Glu166 and Lys73 in a Concerted Base Promotion of Ser70. *J. Am. Chem. Soc.* **2005**, *127* (44), 15397−15407.
(32) Knox, J. R. Extended-Spectrum and Inhibitor-Resistant TEM-Type Beta-Lactamases: Mutations, Specificity, and Three-Dimensional Structure. *Antimicrob. Agents Chemother.* **1995**, *39* (12), 2593−2601.
(33) Kuzin, A. P.; Liu, H.; Kelly, J. A.; Knox, J. R. Binding of Cephalothin and Cefotaxime to D-Ala-D-Ala-Peptidase Reveals a Functional Basis of a Natural Mutation in a Low-Affinity Penicillin-Binding Protein and in Extended-Spectrum.Beta.-Lactamases. *Biochemistry* **1995**, *34* (29), 9532−9540.
(34) Nicoll, C. R.; Massari, M.; Fraaije, M. W.; Mascotti, M. L.; Mattevi, A. Impact of Ancestral Sequence Reconstruction on Mechanistic and Structural Enzymology. *Curr. Opin. Struct. Biol.* **2023**, *82*, No. 102669.
(35) Whittington, A. C.; Kamalaldinezabadi, S.; Santiago, J. I.; Miller, B. G. Vertical Investigations of Enzyme Evolution Using Ancestral Sequence Reconstruction. In *Comprehensive Natural Products III*; Elsevier, 2020; pp 640−653. .
(36) Harms, M. J.; Thornton, J. W. Evolutionary Biochemistry: Revealing the Historical and Physical Causes of Protein Properties. *Nat. Rev. Genet.* **2013**, *14* (8), 559−571.
(37) Hochberg, G. K. A.; Thornton, J. W. Reconstructing Ancient Proteins to Understand the Causes of Structure and Function. *Annu. Rev. Biophys.* **2017**, *46* (1), 247−269.
(38) Siddiq, M. A.; Hochberg, G. K.; Thornton, J. W. Evolution of Protein Specificity: Insights from Ancestral Protein Reconstruction. *Curr. Opin. Struct. Biol.* **2017**, *47*, 113−122.
(39) Modi, T.; Campitelli, P.; Kazan, I. C.; Ozkan, S. B. Protein Folding Stability and Binding Interactions through the Lens of Evolution: A Dynamical Perspective. *Curr. Opin. Struct. Biol.* **2021**, *66*, 207−215.
(40) Campitelli, P.; Modi, T.; Kumar, S.; Ozkan, S. B. The Role of Conformational Dynamics and Allostery in Modulating Protein Evolution. *Annu. Rev. Biophys.* **2020**, *49* (1), 267−288.

https://doi.org/10.1021/acs.jpcb.4c06689
J. Phys. Chem. B 2024, 128, 11658−11665

(41) Modi, T.; Ozkan, S. B. Mutations Utilize Dynamic Allostery to Confer Resistance in TEM-1 β-Lactamase. *Int. J. Mol. Sci.* **2018**, *19* (12), 3808.
(42) Knies, J.; Cai, F.; Weinreich, D. M. Enzyme Efficiency but Not Thermostability Drives Cefotaxime Resistance Evolution in TEM-1 β-Lactamase. *Mol. Biol. Evol.* **2017**, msx053.
(43) Zimmerman, M. I.; Hart, K. M.; Sibbald, C. A.; Frederick, T. E.; Jimah, J. R.; Knoverek, C. R.; Tolia, N. H.; Bowman, G. R. Prediction of New Stabilizing Mutations Based on Mechanistic Insights from Markov State Models. *ACS Cent. Sci.* **2017**, *3* (12), 1311−1321.
(44) Cortina, G. A.; Kasson, P. M. Predicting Allostery and Microbial Drug Resistance with Molecular Simulations. *Curr. Opin. Struct. Biol.* **2018**, *52*, 80−86.
(45) Cortina, G. A.; Kasson, P. M. Excess Positional Mutual Information Predicts Both Local and Allosteric Mutations Affecting Beta Lactamase Drug Resistance. *Bioinformatics* **2016**, *32* (22), 3420−3427.
(46) Risso, V. A.; Sanchez-Ruiz, J. M.; Ozkan, S. B. Biotechnological and Protein-Engineering Implications of Ancestral Protein Resurrection. *Curr. Opin. Struct. Biol.* **2018**, *51*, 106−115.
(47) Keshri, V.; Panda, A.; Levasseur, A.; Rolain, J.-M.; Pontarotti, P.; Raoult, D. Phylogenomic Analysis of β-Lactamase in Archaea and Bacteria Enables the Identification of Putative New Members. *Genome Biol. Evol.* **2018**, *10* (4), 1106−1114.
(48) Pabis, A.; Risso, V. A.; Sanchez-Ruiz, J. M.; Kamerlin, S. C. Cooperativity and Flexibility in Enzyme Evolution. *Curr. Opin. Struct. Biol.* **2018**, *48*, 83−92.
(49) Risso, V. A.; Manssour-Triedo, F.; Delgado-Delgado, A.; Arco, R.; Barroso-delJesus, A.; Ingles-Prieto, A.; Godoy-Ruiz, R.; Gavira, J. A.; Gaucher, E. A.; Ibarra-Molero, B.; et al. Mutational Studies on Resurrected Ancestral Proteins Reveal Conservation of Site-Specific Amino Acid Preferences throughout Evolutionary History. *Mol. Biol. Evol.* **2015**, *32* (2), 440−455.
(50) Harijan, R. K.; Zoi, I.; Antoniou, D.; Schwartz, S. D.; Schramm, V. L. Inverse Enzyme Isotope Effects in Human Purine Nucleoside Phosphorylase with Heavy Asparagine Labels. *Proc. Natl. Acad. Sci. U. S. A.* **2018**, *115* (27), 2609−2616.
(51) Harijan, R. K.; Zoi, I.; Antoniou, D.; Schwartz, S. D.; Schramm, V. L. Catalytic-Site Design for Inverse Heavy-Enzyme Isotope Effects in Human Purine Nucleoside Phosphorylase. *Proc. Natl. Acad. Sci. U. S. A.* **2017**, *114* (25), 6456−6461.

https://doi.org/10.1021/acs.jpcb.4c06689
J. Phys. Chem. B 2024, 128, 11658−11665